

Wearable Passive Cable-Driven Wrist Rehabilitation Robot: Design and Preliminary Experiments

Original

Wearable Passive Cable-Driven Wrist Rehabilitation Robot: Design and Preliminary Experiments / Botta, Andrea; Quaglia, Giuseppe; Takeda, Yukio. - STAMPA. - 147:(2023), pp. 103-112. (16th IFToMM World Congress 2023 Tokyo (JP) November 5-9 2023) [10.1007/978-3-031-45705-0_11].

Availability:

This version is available at: 11583/2983796 since: 2023-11-13T10:27:50Z

Publisher:

Springer Nature Switzerland

Published

DOI:10.1007/978-3-031-45705-0_11

Terms of use:

This article is made available under terms and conditions as specified in the corresponding bibliographic description in the repository

Publisher copyright

Springer postprint/Author's Accepted Manuscript

This version of the article has been accepted for publication, after peer review (when applicable) and is subject to Springer Nature's AM terms of use, but is not the Version of Record and does not reflect post-acceptance improvements, or any corrections. The Version of Record is available online at: http://dx.doi.org/10.1007/978-3-031-45705-0_11

(Article begins on next page)

Wearable Passive Cable-Driven Wrist Rehabilitation Robot: Design and Preliminary Experiments

Andrea Botta^{1,2}, Giuseppe Quaglia¹, and Yukio Takeda²

¹ Department of Mechanical and Aerospace Engineering, Politecnico di Torino, Corso Duca degli Abruzzi 24, Torino 10129, ITALY
{andrea.botta; giuseppe.quaglia}@polito.it

² Department of Mechanical Engineering, Tokyo Institute of Technology, 2-12-1 Ookayama, Meguro-ku, Tokyo 152-8550, JAPAN
takeda.y.aa@m.titech.ac.jp

Abstract. The subject of this investigation is RehaWrist.q, a wearable wrist rehabilitation robot with 3 degrees of freedom (DoF), characterised by its small size, lightweight, and lack of external support structures. The effectiveness of the robot design is assessed through a dedicated passive configuration along with an experimental setup. The robot workspace is suitable for rehabilitation exercises, albeit falling short of the maximum range of motion achievable by a healthy individual. The study underlines the potential of the overall concept, but recommends the implementation of an active actuation system that continuously and automatically adjusts cable tension to fully exploit the device's capabilities.

Keywords: wrist rehabilitation, robotic rehabilitation, cable-driven robot, SDG3

1 Introduction

According to the World Health Organization's (WHO) report on disabilities, around 15% of the world's population has some form of impairment, with 2-4% experiencing major difficulties in functioning [9]. This global estimate of disability is increasing due to the ageing of the population.

Hand and wrist injuries can cause severe disability that affects both social and vocational activities. [3]. Hand trauma occurs globally with high incidence; however, the resulting impairment and disability depend on the severity of the injury, timely diagnosis and adequate treatment [3]. These injuries require a long and repetitive rehabilitation process for the hand to regain its functionality [1].

Robotic rehabilitation has been proposed to overcome the general lack of medical staff by repeating therapeutic movements without the direct involvement of a therapist, so much so that clinical trials conducted by Kwakkel *et al.* and Reinkesmeyer *et al.* [6, 8] confirmed that this approach is effective in supporting the rehabilitation.

In response to these fundamental challenges, the authors have proposed a 3 DoF cable-guided end-effector system that is also wearable, small, lightweight, and does not require external support, named RehaWrist.q [2].

2 Proposed Wrist Rehabilitation Robot

2.1 Wrist Kinesiology

The human wrist is a fairly complex joint that enables the flexion-extension (FE) motion β and the radial-ulnar deviation (RUD) motion γ . In addition to that, the pronation-supination (PS) motion α is often taken into consideration for rehabilitation activities although a joint between the forearm and the elbow enables it (Fig. 1).

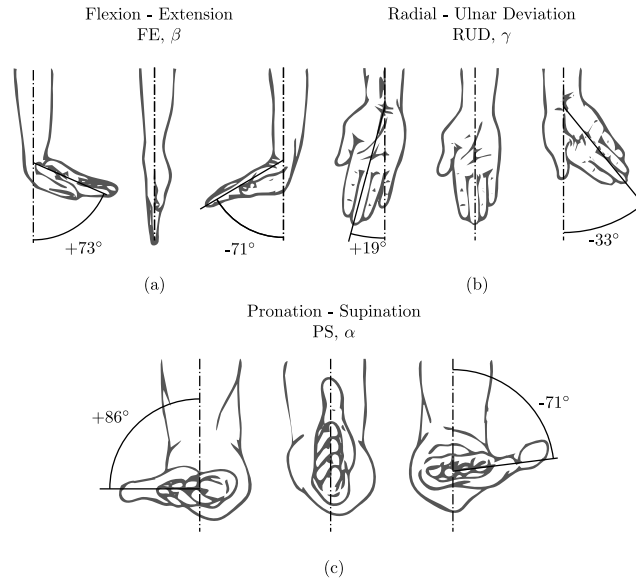


Fig.1: Wrist motions and their maximum range of motion [5]. (a) Flexion - Extension (FE) motion β , (b) Radial - Ulnar Deviation (RUD) motion γ , (c) Pronation - Supination (PS) motion α

The complexity of these joints is primarily due to the fact that the instantaneous centre of rotation is not fixed, but changes depending on the orientation of the hand. As a result, for exoskeleton robots replicating the human joints with external kinematic chains, it is imperative to avoid joint misalignment to avoid hurting the user, as mentioned by Näf *et al.* [7]. Conversely, end-effector robots are attached to the user at only one point, thereby eliminating the issue of joint misalignment. However, these robots may still cause harm by producing

unfeasible motions due to the mismatch between the robot and the user's joints [4].

2.2 Functional Design

The authors developed a cable-driven end-effector rehabilitation robot to avoid any issue related to joint misalignment and to reduce the overall weight as much as possible. Figure 2a is a simplified representation of RehaWrist.q. The robot is made of two platforms connected by four actuated cables to control the user's hand orientation. The fixed platform, which anchor points are A_0 and B_0 , is rigidly linked to the upper arm through a brace-like structure. The forearm is placed inside a cuff that is free to rotate with respect to (w.r.t.) the fixed platform to allow the movement of PS α . To achieve this motion, the forearm cuff is mounted on two curved rails that run in relation to a roller system part of the fixed platform. The user grasps a handle integral to the mobile platform, whose anchor points are A_1 and B_1 . It is possible to generate one of the three motions or a combination of them by properly pulling the right cables. For example, pronation ($\dot{\alpha} < 0$) is obtained by pulling cables $\vec{p}_1 = A_0A_1$ and $\vec{p}_4 = B_0B_1$ and supination ($\dot{\alpha} > 0$) is achieved by pulling cables $\vec{p}_2 = B_0A_1$ and $\vec{p}_3 = A_0B_1$. Similarly, the cable pairs \vec{p}_1 and \vec{p}_3 or \vec{p}_2 and \vec{p}_4 drive the FE motion and the pairs \vec{p}_1 and \vec{p}_2 or \vec{p}_3 and \vec{p}_4 control the RUD motion.

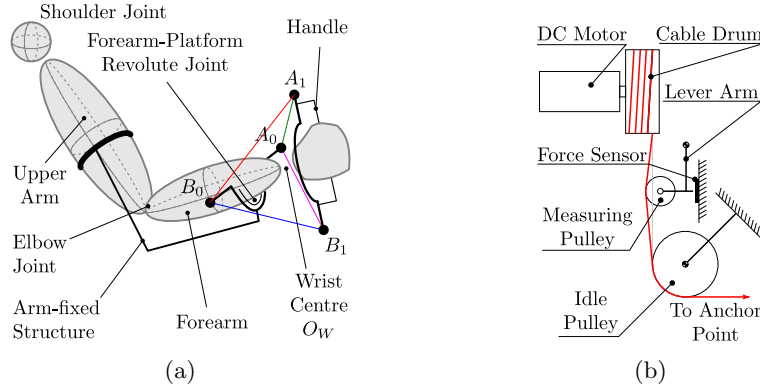


Fig. 2: (a) Functional diagram of the proposed rehabilitation robot. Cable \vec{p}_1 is green, \vec{p}_2 is red, \vec{p}_3 is magenta, and \vec{p}_4 is blue. (b) Functional diagram of the actuation sub-system

Figure 2b illustrates how the robot pulls the cable applying the appropriate tension. Each cable is wound around a drum or pulley coupled to a DC motor shaft and guided to the corresponding anchor point by an idle pulley. Both the motor and the idle pulley are mounted on the fixed platform. Between the two, there is a smaller idle pulley mounted on a lever hinged to the fixed platform

and pushing onto a force sensor that is used to measure the cable tension. A dedicated motor controller ensures that the motor generates the correct torque to apply the required cable tension.

Figure 3 shows the parallel robot alone with its main parameters with the mobile base in two different orientations, namely, the rest position and a generic position. Each platform has a size of L_i , with $i = 0, 1$ where 0 refers to the fixed platform and 1 to the mobile one, and it is placed at a distance d_i from the ideal wrist centre O_W . The platform reference frame $\{O_i\}$ is at its centre.

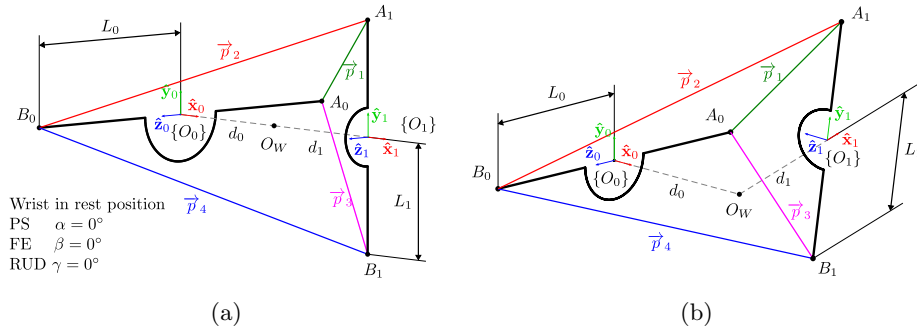


Fig. 3: Diagram of the two platforms and their reference frames in the rest position (a) and in a generic pose (b).

Figure 4a shows a CAD model of the final design, and Fig. 4b depicts the current prototype.

The interested reader may refer to [2] for a detailed description of how the robot was designed and sized to optimise the effective force transmitted to the mobile platform by the cables.

2.3 Passive Configuration

To test and prove the effectiveness of the proposed design, a passive version of the robot was built. Instead of using four motors to drive the cables and, thus, the user's hand, in the passive configuration, the user moves his/her hand against the reaction of four spring-loaded sub-systems that tension the cables to oppose the user's motion.

Figure 5 depicts the spring-loaded sub-systems for two cables, showing one of them in an exploded view. The cable coming from one of the fixed anchor points (A_0 or B_0) is wound on a pulley (not shown) fixed on a shaft (5). A power spring (6) is mounted at the opposite end of the shaft to generate an elastic reaction to oppose the user pulling the corresponding cable. To do so, the outer end of the power spring is attached to a toothed knob (8) whose axial rotation is locked by engaging a toothed spacer (4). To adjust the power spring preload, the knob can be pulled back to disengage from the spacer, then it is rotated to adjust the

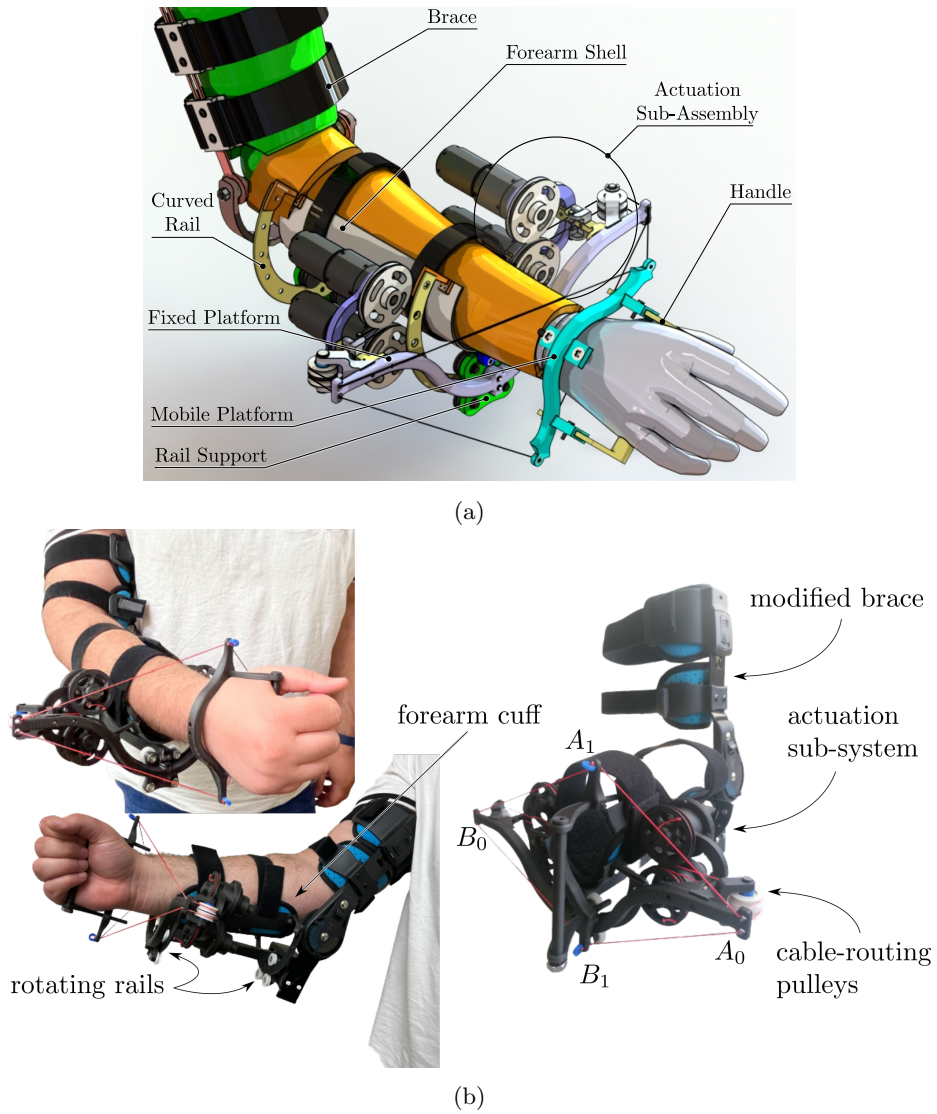


Fig. 4: (a) 3D model of the prototype. (b) Current prototype in the passive configuration

preload and, at last, it is locked back in position by engaging again the toothed spacer with the help of a compression spring (9).

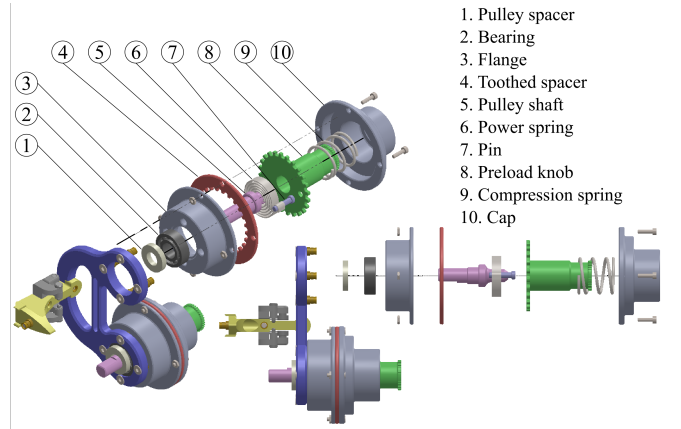


Fig. 5: Isometric and side views of the spring-loaded passive sub-system

3 Preliminary tests

This section reports on the preliminary tests done on RehaWrist.q in the passive configuration to evaluate its wearability, comfort, and functionality. The tests were carried out on a healthy individual (male, 30 years old, right handed).

3.1 Methods

Two 9-axis IMUs (BNO055 by Bosch) were fixed to the mobile and fixed platforms to evaluate their relative orientation, that is, the orientation of the mobile platform w.r.t. the fixed one. Both sensors estimate the corresponding body orientation w.r.t. a generic reference frame $\{N\}$, thus, the relative orientation ${}^0\mathbf{R}_1$ is obtained as

$${}^0\mathbf{R}_1 = {}^N\mathbf{R}_0^{-1} {}^N\mathbf{R}_1 \quad (1)$$

where ${}^N\mathbf{R}_0$ and ${}^N\mathbf{R}_1$ are the orientations of the fixed and mobile platforms w.r.t. the reference frame N , respectively.

A force sensing resistor (FSR05 by Ohmite) is mounted as depicted in Fig. 2b to measure the reaction force applied to the measuring pulley and therefore the tension of the cable.

Knowing the tension of each cable and the orientation of the mobile platform, it is possible to evaluate the net force \vec{F}_1 and torque \vec{T}_1 acting on the hand as

follow

$$\begin{bmatrix} \hat{p}_1 & \hat{p}_2 & \hat{p}_3 & \hat{p}_4 \\ \vec{r}_1 \times \hat{p}_1 & \vec{r}_2 \times \hat{p}_2 & \vec{r}_3 \times \hat{p}_3 & \vec{r}_4 \times \hat{p}_4 \end{bmatrix} \begin{bmatrix} f_1 \\ f_2 \\ f_3 \\ f_4 \end{bmatrix} = \begin{bmatrix} \vec{F}_1 \\ \vec{T}_1 \end{bmatrix} \quad (2)$$

where \hat{p}_i is the direction of the i -th cable, \vec{r}_i is the position of the anchor point of the i -th cable on the mobile platform w.r.t. the wrist centre, and f_i is the tension of the i -th cable.

The tests consisted of setting the cable tension preload to various values and then letting the user perform the three motions in sequence. The objective was to evaluate the effective range of motion (RoM) and the force applied to the cables.

3.2 Results

Figure 6a shows an example of the orientation of the hand measured during a test. During such a test, the user first performed only FE movements (blue-shaded area), then only RUD movements (red-shaded area), and finally only PS movements (green-shaded area). Given all tests, the maximum RoMs observed for PS, FE and RUD were 110° , 93° , and 45° respectively. Compared to the values in [5], PS RoM is 30% smaller, FE is 35% smaller considering the maximum values, RUD is instead 13% smaller. These reduced RoMs are always due to the hand or mobile platform touching one cable or the fixed platform.

Figure 6b and Figure 6c depicts the measured component of \vec{F}_1 and \vec{T}_1 in $\{O_0\}$, obtained with (2). From the force components, it can be noted that there is always an average compression force along the forearm axis (\hat{x}_0 axis) of about 2 N. This happens because the four cable must always be in tension and due to the robot architecture this always produce a wrist compression force. Thus, the usage of this device should be limited to users that would not suffer from an applied wrist compression force. Also, in the initial seconds, it can be observed that the force component along \hat{y}_0 and \hat{z}_0 are non-zero due to an asymmetric setup of the tension of the four cables. In Fig. 6c can be observed that for both PS and FE ($T_{1,x}$ and $T_{1,y}$), it is possible to comfortably feel an opposing torque up to 0.5 N, but higher values can be reached too if the device is properly setup to favour one motion. The opposing torque during RUD is instead much smaller because the RoM and thus the displacement of the cables is significantly smaller than in the other two cases.

Although the device cannot cover the full RoM of the three movements, the resulting RoMs are more than enough for rehabilitation exercises. In the proposed passive configuration, the hand is not guided by the mobile platform in its movements, but instead the opposite occurs. Thus, the resulting motion is often a combination of PS, FE, and RUD, as seen during the RUD phase in Fig. 6a.

The passive configuration showed some expected drawbacks. With this configuration, instead of an active one where each cable is driven by a motor, it is

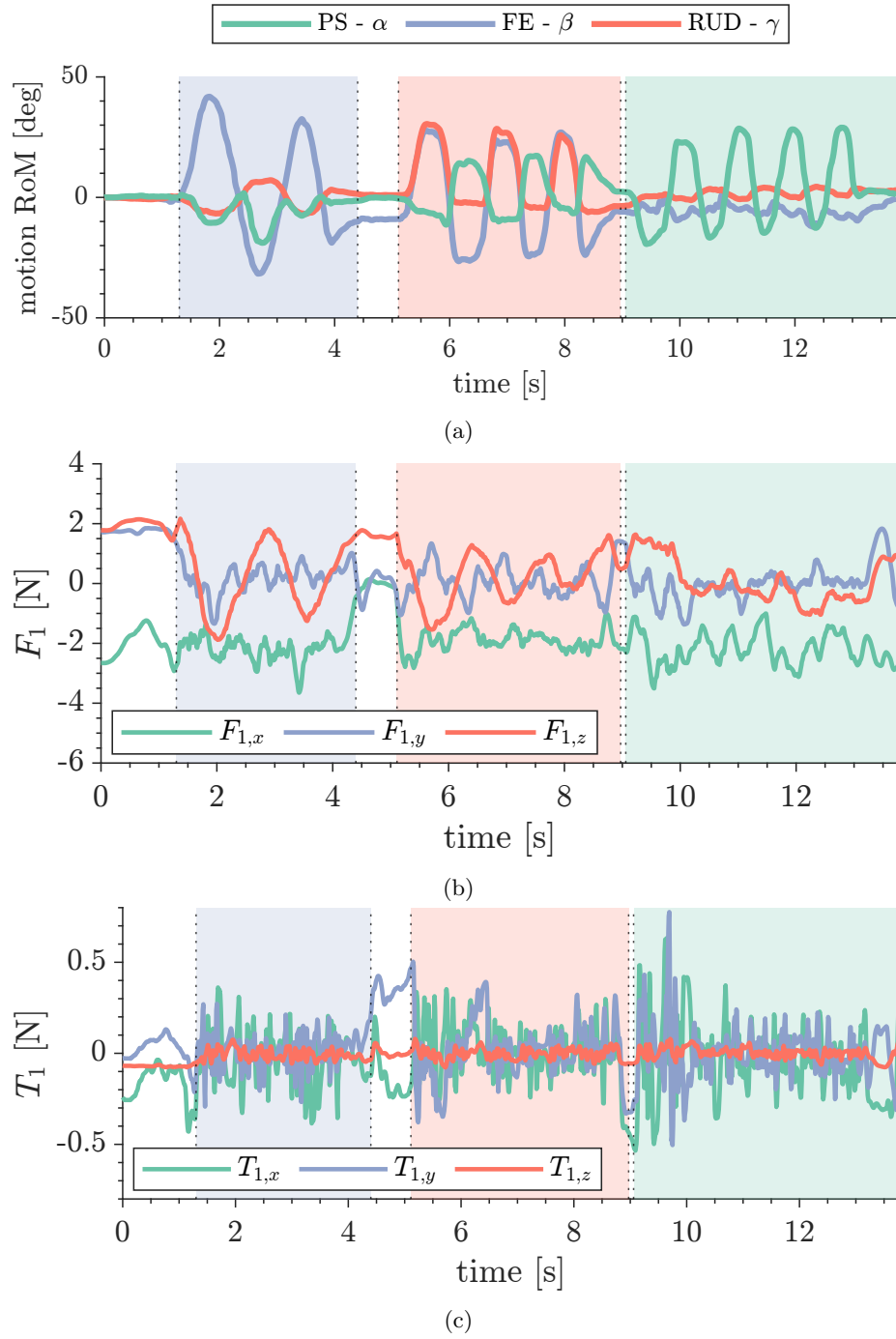


Fig. 6: (a) Orientation of the hand w.r.t. the forearm during a test. (b) Component of \vec{F}_1 . (c) Component of \vec{T}_1 .

practically impossible to properly adjust the cable tension while using the device. Also, because the springs can apply tension to the elongating cables, each unique motion should require a dedicated setup to guarantee that each cable is always in tension. This means that at least six different setups are needed, two for each movement. Using a non-optimal setup simply means that the actual RoM where proper resistance is applied is reduced. Nevertheless, the device is able to provide light to medium resistance to user rehabilitation movements. For PS motions it is easier to achieve the largest resisting torque due to the largest force lever arm, while FE and RUD motions produce significantly lower resisting torques using the same initial setup. This proves again how a dedicated setup is required for each movement.

Another limitation is the presence of a non-zero compression force acting on the wrist. Therefore, this device may not be suitable for some users because it may cause additional harm to the wrist joint. Also, this means that this device requires a proper interface between the hand and the mobile platform to better distribute this load.

4 Conclusions

This study showcases a wearable cable-driven wrist rehabilitation robot, specifically its passive configuration where power springs are used to tension the robot cables. This configuration of the proposed robot has been built and tested to evaluate its core functionality regardless of the actuation system. A dedicated experimental setup has been implemented to evaluate the range of motion of the robot and the tensions of the cables. Several tests were performed by a user repeating the three basic motions in sequence.

Despite its limitations, the robot proved to be suitable for rehabilitation exercises, although it cannot match a healthy person's maximum range of motion. As expected, the use of springs instead of motors to tension the cables led to some issues, requiring a unique setup for each motion to ensure that the cables are not loose. However, the robot generates light to medium resisting torques, which allows the user to exercise effectively.

Overall, the results demonstrate the robot abilities and potential for rehabilitation exercises. An active actuation system that continuously and automatically adjusts cable tension is necessary to exploit this device potential and enhance the robot performance.

Acknowledgment

This work was developed with the support of the Japan Society for the Promotion of Science (JSPS) Postdoctoral Fellowships for Research in Japan.

References

1. Albanese, G.A., Marini, F., Taglione, E., Gasparini, C., Grandi, S., Pettinelli, F., Sardelli, C., Catitti, P., Sandini, G., Masia, L., Zenzeri, J.: Assessment of human

- wrist rigidity and pain in post-traumatic patients. In: 2019 IEEE 16th International Conference on Rehabilitation Robotics (ICORR), pp. 89–94 (2019). DOI 10.1109/ICORR.2019.8779508. ISSN: 1945-7901
2. Colucci, G., Botta, A., Verutti, M., Visconte, C., Quaglia, G., Liu, Y.C., Takeda, Y.: A preliminary synthesis of a light and compact wearable cable-driven parallel robot for wrist joint rehabilitation. In: Proceedings of Jc-IFToMM International Symposium, vol. 5, pp. 57–64. Japanese Council of IFToMM, Yokohama (2022). DOI 10.57272/jciftomm.5.0_57. URL https://www.jstage.jst.go.jp/article/jciftomm/5/0/5_57/_article
 3. Crowe, C.S., et al.: Global trends of hand and wrist trauma: a systematic analysis of fracture and digit amputation using the Global Burden of Disease 2017 Study. *Injury Prevention* **26**(Suppl 2), i115–i124 (2020). DOI 10.1136/injuryprev-2019-043495. URL <https://injuryprevention.bmj.com/content/26/Suppl.2/i115>. Publisher: BMJ Publishing Group Ltd Section: Original research
 4. Hussain, S., Jamwal, P.K., Van Vliet, P., Ghayesh, M.H.: State-of-the-Art Robotic Devices for Wrist Rehabilitation: Design and Control Aspects. *IEEE Transactions on Human-Machine Systems* **50**(5), 361–372 (2020). DOI 10.1109/THMS.2020.2976905. Conference Name: IEEE Transactions on Human-Machine Systems
 5. Kapandji, I.A.: *The Physiology of the Joints, Volume 1: Upper Limb, Volume 1, 5th edition* edn. Churchill Livingstone, Edinburgh (2007)
 6. Kwakkel, G., Kollen, B.J., Krebs, H.I.: Effects of Robot-Assisted Therapy on Upper Limb Recovery After Stroke: A Systematic Review. *Neurorehabilitation and Neural Repair* **22**(2), 111–121 (2008). DOI 10.1177/1545968307305457. URL <https://doi.org/10.1177/1545968307305457>. Publisher: SAGE Publications Inc STM
 7. Näf, M.B., Junius, K., Rossini, M., Rodriguez-Guerrero, C., Vanderborght, B., Lefeber, D.: Misalignment Compensation for Full Human-Exoskeleton Kinematic Compatibility: State of the Art and Evaluation. *Applied Mechanics Reviews* **70**(5) (2019). DOI 10.1115/1.4042523. URL <https://doi.org/10.1115/1.4042523>
 8. Reinkensmeyer, D.J., Kahn, L.E., Averbuch, M., McKenna-Cole, A., Schmit, B.D., Rymer, W.Z.: Understanding and treating arm movement impairment after chronic brain injury: progress with the ARM guide. *Journal of rehabilitation research and development* **37**(6), 653–662 (2014). URL <https://escholarship.org/uc/item/65z7c4s7>
 9. World Health Organization: World report on disability 2011. World Health Organization (2011)